

RESPONSE SURFACE METHODOLOGY APPLIED TO ELECTRO-FENTON PROCESS FOR DEGRADATION OF RED BEMACID AS TEXTILE DYE MODEL

KELTHOUM MAAMAR,* CHAHINAZ FARES,** IZZEDINE SAMEUT BOUHAÏK,*** LARBI MAHMOUDI,* BASSAM MUTHANNA**** and MUSTAPHA DOUANI*

*Laboratory of Plant Chemistry-Water-Energy, Process Engineering Department, Faculty of Technology, Hassiba Benbouali University of Chlef, Esalem City, 02000, Chlef, Algeria

**Faculty of Technology, Hassiba Benbouali University of Chlef, Chlef, Algeria

***University of Chlef, LPTPM, Esalem City, 02000, Chlef, Algeria

****Department of Mechanics, Faculty of Technology, Saad Dahlab University of Blida 1, Blida, Algeria

✉ Corresponding author: K. Maamar, k.maamar@univ-chlef.dz

Received July 10, 2023

The textile industry produces persistent organic pollutants (POPs) that pose significant risks to ecosystems because of their toxic and hazardous nature. Consequently, there is an urgent requirement for the development of effective techniques to treat the effluents and remove these compounds. This work studied the viability of the Electro-Fenton (EF) process as a potential alternative for treating textile wastewater contaminated with POPs. A batch electrochemical reactor, equipped with a platinum grid cathode and stainless-steel sacrificial anode, was utilized to eliminate Red Bemacid (RB) dye. The study investigated the impact of four key operational parameters: (i) stirring speed (rpm), (ii) oxygen flow rate (L/min), (iii) supporting electrolyte concentration [Na₂SO₄] (mg/L), and (iv) current intensity (A), as well as their interactions on RB removal. To perform this, Central Composite Experimental Design (CCD) and Response Surface Methodology (RSM) were employed. Under optimized EF conditions for RB removal (stirring speed = 205.09 rpm, oxygen flow rate = 0.20 L/min, current intensity = 0.306 A, and supporting electrolyte concentration = 0.09 M), the EF process demonstrated exceptional removal efficiency, achieving approximately 94.51% removal of RB. The obtained results showed that the kinetic data of RB removal were in good agreement with the Behnjady-Modirshahla-Ghanbery (BMG) model. The CCD analysis revealed that the main effect of the current intensity had a significant impact on RB removal, as well as the interaction of all paired variables.

Keywords: wastewater, Electro-Fenton (EF), Red Bemacid (RB), hydroxyl radicals (OH[•]), Central Composite Design (CCD)

INTRODUCTION

Generally, the continuous release of synthetic dyes from different types of manufacturing industries, such as cosmetic, printing, industrial pharmaceutical, food colorants, paper production, plastics, leather, and textile, is highly undesirable due to the persistent nature of the resulting colored effluents. These effluents have the ability to persist in the environment for extended periods of time, posing a significant threat to ecosystems and human health.¹⁻⁴ The discharge of effluents containing synthetic dyes into water resources presents serious risks to both human well-being and the delicate balance of the aquatic ecosystem.

This is primarily due to the complex and harmful properties exhibited by these dyes, including carcinogenicity, toxicity, and persistence. The harmful effects of synthetic dyes extend beyond human health, with long-lasting detrimental impacts on aquatic life.²⁻⁷ Moreover, the treatment of textile waste, a major contributor to such effluents, has become increasingly challenging, posing a significant obstacle for researchers and industrialists in effectively addressing the treatment and mitigation of these hazardous substances.^{2,7-8}

Over the past two decades, Advanced Oxidation Processes (AOPs) have emerged as effective methods for degrading non-biodegradable organic compounds in water, particularly those with complex and inert characteristics.^{9,10} These techniques utilize highly reactive hydroxyl radicals (OH•) to efficiently attack and oxidize refractory contaminants, leading to the degradation of persistent organic matter with large and intricate structures.^{7,10-12}

Among the AOPs, the Electro-Fenton (EF) process is recognized as an environmentally friendly, cost-effective, efficient, and promising technology for the removal of persistent organic pollutants (POPs).^{10,12-13} It involves the continuous *in situ* electro-generation of Fenton's reagents (hydrogen peroxide and ferrous ions), which serve as precursors for hydroxyl radicals. The formation of hydroxyl radicals occurs through the reaction between ferrous ions and hydrogen peroxide, as shown in the following Equation (1):¹⁴⁻¹⁷



Several combinations were developed to generate Fenton's reagent:¹⁸⁻¹⁹

- EF-H₂O₂: H₂O₂ is generated at cathode by two-electron reduction of dissolved oxygen,¹⁹⁻²⁰ while Fe²⁺ is added externally to the process;²¹
- Addition of EF-reagents: Both species H₂O₂ and Fe²⁺ are externally added to the electrolytic cell from outside;^{18,22}
- Ferred-Fenton process: Fe²⁺ is produced at cathode by Fe³⁺ reduction, but H₂O₂ is externally added in solution;
- Addition of Fe³⁺: Fe³⁺ is externally added, and Fenton's reagents are electro-generated via cathodic reduction;
- EF-Feox method: H₂O₂ is externally added, whereas Fe²⁺ is continuously provided by oxidation at anode;^{1,8,18,20,23}
- Electrochemical generation of Fenton's reagent (Fe²⁺ and H₂O₂): Fe²⁺ is generated at sacrificial anode and H₂O₂ is generated by a reduction of dissolved oxygen at cathode.^{1,8,19,20,24}

The stringency of the EF process is defined by the control of various factors: (i) factors governing the electrochemical process, (ii) factors governing the electro-generation of Fenton's reagent, and (iii) factors controlling the reaction mechanism of organic matter degradation. However, the complexity of the process may require optimization of the factors governing Fenton's reagent generation, while maintaining

constant parameters of the electrochemical cell that were initially optimized, such as voltage, electrolyte nature, current density, and initial dye concentration.

Several researchers have applied EF technology to treat refractory effluents, including dyes, pesticides, and anti-inflammatory pharmaceuticals. These studies have demonstrated the remarkable efficiency of the EF technique in degrading such effluents.²⁵⁻³⁰ Do *et al.* have used the EF process to remove residual dye products, employing magnetite coated metallic foams as a cathode. They have observed a removal efficiency of 95.2% at 50 ppm after 120 minutes of electrolysis, and an exceptional removal efficiency of 99.8% was achieved at 100 ppm after 60 minutes of electrolysis.² The application of the EF process for treating real dyeing wastewater using an activated carbon fibre cathode was performed by Wang *et al.*²⁵ Their results showed that the achieved COD removal efficiency was 75.2% under the current density of 3.2 mA/cm².²⁵ Ghoneim *et al.*²⁶ have studied the EF oxidation of aggressive water soluble Sunset Yellow FCF azo-dye using an RVC cathode. Their analysis revealed that the mineralization of pollutant reached 97% after 2 hours of reaction.²⁶ On the other hand, the EF process was also used by M. Panizza *et al.*²⁷ in order to degrade Alizarin Red using a gas-diffusion cathode for producing hydrogen peroxide. Their analyses proved that the COD removal in the presence of ferrous ion has significant results, and may reach up to or exceed 90%. However, in the absence of ferrous ions, the COD removal was 45%.²⁷

In this study, Response Surface Methodology (RSM) was applied using a Central Composite Design (CCD) to investigate the main effects of variables controlling the interaction of Fenton's reagents with an organic dye-based pollutant and to optimize the process variables for Fenton reagent regeneration and dye removal. Furthermore, four independent variables were examined: supporting electrolyte concentration (mg/L) [Na₂SO₄], oxygen flow rate (L/min), stirring speed (rpm), and current intensity (A). The response function (dependent variable) was the decolorization efficiency of Red Bemacid (RB) dye, Y (%), by the EF process, measured using UV-Vis spectroscopy. Correlations were found between the independent and dependent variables, contributing to the understanding of factors influencing the electro-generation of Fenton's reagent and, consequently, factors

improving the degradation mechanism of the RB reaction. The optimum values of the corresponding EF process variables were also predicted by CCD.

EXPERIMENTAL

Chemical analysis

The RB dye ($C_{24}H_{20}ClN_4NaO_6S_2$) used in this study was provided by a textile company from the West of Algeria. Sulfuric acid and sodium hydroxide were both obtained from Merck, of 98% purity, and were utilized for pH adjustment as diluted solutions (1M). Sodium sulphate (95% pure) and sodium chloride with a purity of 98% were used as supporting electrolyte. All solutions were prepared using distilled water at room temperature.

Electrochemical reactor

EF experiments were performed at room temperature of 23 ± 1 °C in a 200 mL batch electrochemical reactor. The reactor was controlled by an adjustable DC power supply unit and the solution was homogenized by agitation ranging from 200 to 800 rpm using a magnetic stirrer. A stainless steel sheet ($4.2 \text{ cm} \times 3.1 \text{ cm} \times 1 \text{ mm}$) was used as the sacrificial anode, while a platinum plate grid ($3 \text{ cm} \times 2.9 \text{ cm} \times 0.5 \text{ mm}$) served as the cathode.^{24,28} During the EF treatment, the pH value of the solution was adjusted between 2.8 and 3.0, by adding either NaOH (1M) or

H_2SO_4 (1M).²⁹ Moreover, the oxygen flow was controlled by a Gilmont Instruments flow meter.

In this study, Fenton's reagents (Fe^{2+} and H_2O_2) were electro-generated. Hydrogen peroxide was accumulated at the cathode by a continuous aeration according to Equation (2).^{2,30-31}



Meanwhile, the Fe^{2+} ions were simultaneously generated through a sacrificial anode and regenerated by the reduction of Fe^{3+} ions at the cathode according to Equation (3) and Equation (4), respectively:^{9,12}



Analytical procedure

All samples of initial and residual dye concentrations were measured spectrophotometrically, using a Shimadzu UV-vis spectrophotometer at the maximum wavelength of the dye, approximately 509 nm. The relation used to calculate the degradation efficiency, Y (%), of Red Bemacid (RB) dye is given by Equation (5):

$$Y(\%) = \frac{C_0 - C_t}{C_0} \times 100 \quad (5)$$

where C_0 and C_t are the initial concentration and the concentration at time t (mg/L), respectively.

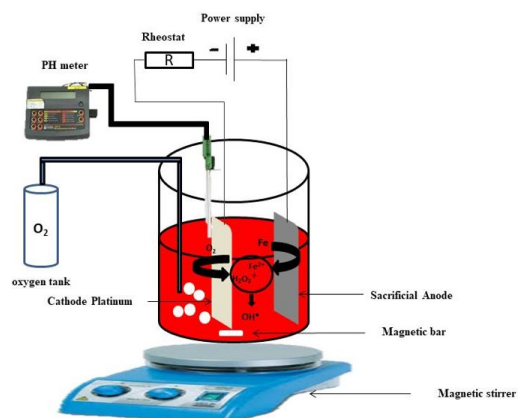


Figure 1: Schematic diagram and photograph of EF experimental system

In order to determine the suitable rate model of RB dye elimination, first and second order models were tested according to the following equations:

- Pseudo-first-order reaction model:

$$\ln\left(\frac{C_0}{C_t}\right) = K_1 \times t \quad (6)$$

- Pseudo-second-order reaction model:

$$\frac{1}{C_t} - \frac{1}{C_0} = K_2 \times t \quad (7)$$

where C_0 and C_t are the initial concentration and the concentration at time t (mg/L), respectively; K_1 and K_2 represent the first-order constant (min^{-1}) and second-order constant ($\text{mg}^{-1} \cdot \text{L} \cdot \text{min}^{-1}$).

The third kinetic model tested was the Behnajady-Modirshahla-Ghanbery model (BMG).³² The linearized form of the BMG model is expressed as:

$$\frac{t}{\left[1 - \frac{C_t}{C_0}\right]} = m + bt \quad (8)$$

where m and b are two constants of this model.

Central Composite Design (CCD)

In general, Response Surface Methodology (RSM) is considered as a collection of different statistical and mathematical processing tools. In addition, this methodology is performed for different applications of empirical model design and analysis in order to display the effects of several factors at different levels on the measured response. Moreover, this technique is used in order to optimize the process and to reduce the number of experimental runs.^{9,33-36} In this study, a CCD was applied to investigate the relation between the independent variables (factors) affecting Fenton’s reagent and the removal efficiency of RB (Y, %), and to determine the optimum values of the operating independent variables. The chosen factors, considered as independent variables: stirring speed (A), oxygen flow (B), current density (C) and Na₂SO₄ concentration (D), the coded levels and the ranges selected for the experimentation were listed in Table 1.^{14,18}

The CCD was divided in three groups of design points:

1. The full factorial – was applied between the low level (-1) and the high level (+1); this design with 2 levels and 4 factors (k) has 2^k runs = 16 runs;
2. The center points – denoted in coded variables as 0; a better variance estimate was evaluated by 3 to 6 repeats of center points; for this study, 6 repeats were used;

3. The axial points called star points – each variable was placed at ± α and all other factors were at zero. Further selection of the Face-Centered Design in CCD sets the value of α (the distance of the axial point from the center) to ±1.³⁷ Thus, the position of axial points stands within the factorial region.^{14,18} The number of the axial points was 8.

Therefore, a total of 30 trials were used for this study and the design matrix was developed in Table 2. The interaction effects are calculated by multiplying two or more independent variables. The response of the decolorization efficiency of RB dye, Y (%), analyzed by the UV-Vis spectrophotometer, was listed in Table 2. The experimental data fitted into a generated polynomial model between the dependent variable (or response) Y and independent variables (or factors) has the form of Equation (9):

$$Y = a_0 + a_1A + a_2B + a_3C + a_4D + a_{12}AB + a_{13}AC + a_{14}AD + a_{23}BC + a_{24}BD + a_{34}CD + a_{11}A^2 + a_{22}B^2 + a_{33}C^2 + a_{44}D^2 + a_{123}ABC + a_{124}ABD + a_{134}ACD + a_{234}BCD$$

where a₀: constant term, a_i: linear coefficients for independent variables, a_{ij}: quadratic term coefficient, a_{ij}: interactive term coefficient; and a_{ijk}: higher-order interaction coefficients. This polynomial model (objective function) was optimized by quadratic programming³⁸ to find the operating parameters that maximize the RB removal rate.

Table 1
Input EF variables and their ranges

Independent variable	Range and level				
	Lowest limit -α (-1)	Lower limit (-1)	Center point (0)	Higer limit (1)	Highest limit +α (1)
A: stirring speed (rpm)	200	200	500	800	800
B: Oxygen flow (L/min)	0.2	0.2	0.3	0.4	0.4
C: Current intensity (A)	0.2	0.2	0.3	0.4	0.4
D: [Na ₂ SO ₄] (mg/L)	0.05	0.05	0.075	0.1	0.1

Table 2
Experimental variable-based matrix of CCD and results of RB removal

Run	Factors				Response
	A	B	C	D	Y (%)
1	-1	-1	-1	-1	50.21
2	1	-1	-1	-1	38.7
3	-1	1	-1	-1	40.03
4	1	1	-1	-1	37.05
5	-1	-1	1	-1	60.35
6	1	-1	1	-1	40.315
7	-1	1	1	-1	53.105
8	1	1	1	-1	70
9	-1	-1	-1	1	58
10	1	-1	-1	1	49.68

11	-1	1	-1	1	45.6
12	1	1	-1	1	62.53
13	-1	-1	1	1	77.947
14	1	-1	1	1	70.85
15	-1	1	1	1	72.05
16	1	1	1	1	90.63
17	0	0	0	0	85.5
18	0	0	0	0	85.9
19	0	0	0	0	85.87
20	0	0	0	0	85.5
21	0	0	0	0	85.9
22	0	0	0	0	85.87
23	0	0	1	0	66.86
24	-1	0	0	0	85.62
25	0	0	-1	0	47.72
26	0	0	0	1	94.38
27	0	1	0	0	87.32
28	1	0	0	0	85.89
29	0	0	0	-1	77.14
30	0	-1	0	0	84.19

RESULTS AND DISCUSSION

Results of preliminary tests

To emphasize the variables influencing the electro-generation of the Fenton reagent, which is essential for the degradation of organic matter, preliminary tests were conducted to optimize the parameters of the electrochemical cell (voltage,

nature of the electrolyte, and initial concentration of the dye).

In this study, the first electrochemical variable tested was the nature of the supporting electrolyte. The addition of this electrolyte is required to improve the conductivity of the solution containing an organic pollutant.

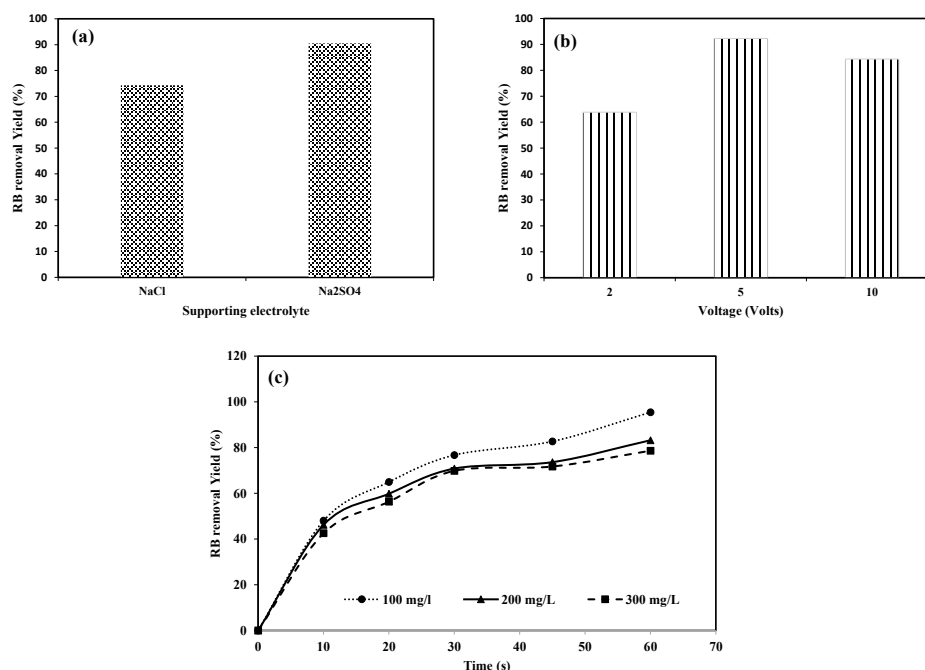


Figure 2: Results of preliminary tests: (a) Effect of supporting electrolyte (time = 60 min; initial RB concentration = 100 mg/L; solution pH 3); (b) Effect of voltage (time = 60 min; CI = 400 mA, solution pH 3); (c) Effect of current intensity (solution pH = inherent (3))

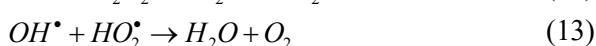
Sodium sulfate (Na₂SO₄) and sodium chloride (NaCl) were examined as supporting electrolytes,

as both of these supporting electrolytes are frequently and commonly used in most literature

studies.²¹ As illustrated in a study using the same electrical power, the addition of Na₂SO₄ led to an increased RB elimination efficiency (91.50%), compared to the addition of NaCl (74.26%). This decrease in the presence of NaCl electrolyte could be attributed to the formation of reaction intermediates, specifically through the reaction between chloride ions (Cl⁻) and hydroxyl radicals (OH•), chloride ions can act as scavengers of hydroxyl radicals.³¹



In an EF system, the applied voltage is an important factor that greatly influences the generation of hydrogen peroxide at the cathode. Moreover, an increase in the voltage leads to an accumulation of OH• and consequently enhances the elimination of organic pollutants. Figure 2b displays the RB removal due to the EF process at diverse voltages. In addition, an increase in RB removal efficiency up to 91.2% is observed at an applied voltage of 5 V. Beyond 5 V, a decrease in RB degradation is detected, likely due to the excessive generation of hydrogen peroxide resulting from the recombination of OH• (Eq. 11) and the reaction between H₂O₂ and OH• (Eq. 12), leading to the formation of reaction intermediates.^{1,20}



Generally, the efficiency of pollutant removal depends on its initial concentration. An inversely proportional relationship between the initial concentration of dye and the efficiency of the EF process is observed for three initial concentrations of RB solutions (100, 200, and 500 mg/L), as shown in Figure 2c. The obtained results demonstrate that the degradation rate of RB dye decreases with increasing initial concentrations. Consequently, this result can be explained by the need for a large number of hydroxyl radicals to eliminate the high concentrations of the contaminant.¹¹ Indeed, the results show that the EF process, under adequate conditions, achieves the highest removal value of 95% for RB dye after 60 minutes at an initial concentration of 100 mg/L.

The electrochemical cell variables were optimized from preliminary tests and were utilized in this work to show the influence of electro-generation factors of the Fenton reagent, which is essential for organic matter degradation.

However, the optimized parameters are as follows: the nature of the supporting electrolyte: Na₂SO₄; voltage: 5 V, and initial concentration of the pollutant (RB dye): 100 mg/L.

Kinetic analysis of RB degradation

The BMG model is considered essential for predicting the rate of RB dye degradation, providing a comprehensive understanding of the efficiency of the oxidation process. RB dye is oxidized by OH• radicals, following the kinetics of the BMG model ($R^2 > 0.96$), as shown in Table 3.

The values of K_{app} and linear correlation (R^2) from pseudo-first- and pseudo-second-order kinetics are presented in Table 3. K_1 and K_2 represent the apparent pseudo-first- and pseudo-second-order reaction constants, respectively. All the values of rate constants, K_1 and K_2 , for the elimination of RB dye under the corresponding operating conditions fixed above by EF, were analytically determined from the slope of $\ln(C_0/C_t)$ against process t , and $1/C_t - 1/C_0$ against t , respectively. Based on the correlation coefficients (R^2) indicated in Table 3, the experimental data better align with the pseudo-first-order reaction mechanism (as evidenced by high R^2 values). Thus, the obtained results presented in Table 3 demonstrate that an increase in the initial concentration of RB dye leads to a decrease in the pseudo-first-order rate constants. This action can be explained by the performance acceleration of the competitive reactions between the oxidizing RB dye by-products forming during the EF process and hydroxyl free radicals.¹

According to the values of correlation coefficient (R^2) illustrated in Table 3, the BMG model exhibits the highest R^2 values, indicating that the experimental data are better fitted by the BMG kinetic model. The degradation reaction occurs in two stages: a fast rate stage, followed by a slower second stage, as shown in Figure 2c. These two stages are characterized by the values of $1/m$ and $1/b$, which represent the initial reaction rate and the maximum reaction fraction, respectively.³⁹⁻⁴⁰

Response Surface Methodology analysis

The Central Composite Face-centered (CCF) design was used to fit the second-order model and determine the optimum process factors (variables) that influence the electro-generation of the Fenton's reagent, consequently affecting the removal of RB dye.

Depending on the results of multiple validation tests (Table 4), analyzing the experimental data, the quadratic model was classified to be the best fitting model. Furthermore, the adequacy of this model which is established by ANOVA analysis,

was confirmed by the correlation coefficient determination ($R^2 = 0.99$) and the adjusted determination coefficient ($R^2_{Adj} = 0.973$), which is greater than 0.8.⁴¹

Table 3
Kinetic parameters for elimination of RB dye at different initial concentrations

Red Bemacid dye concentration (mg/L)	Pseudo-first order		Pseudo-second order		BMG model		
	K_1	R^2	K_2	R^2	1/m	1/b	R^2
100 mg/L	0.0459	0.9499	0.003	0.7204	0.9891	0.1537	0.9647
200 mg/L	0.0297	0.9252	0.0004	0.9579	0.8604	0.1539	0.9735
500 mg/L	0.0238	0.9029	0.0001	0.9737	0.8266	0.1414	0.9734

Moreover, the statistical significance of Fisher test (F-test) calculated from the experimental data ($F\text{-test}_{\text{calculated}} = 26179.74$) (Table 5) is much greater than the tabulated critical F-value ($F_{\text{critical value}} = 2.78$ at 95% confidence level), indicating that the null hypothesis was rejected in favour of the alternative hypothesis.

Due to the lack of a fitting test, the P_{value} was found to be greater than the significance level ($\alpha = 0.05$). As a result, the model was considered statistically significant at the 95% confidence level, and the selected model (Eq. (9)) was deemed sufficient to describe the experimental data. The coefficients of the model are provided in Table 5.

The analysis of variance (ANOVA) for RB dye removal by CCF was presented in Table 5. Variables with a P_{value} less than 0.05 indicate that these terms are statistically significant.¹⁴ To simplify the correlation between the variables and the response, Equation (9) was reduced to a second-order polynomial equation, as given in Equation (13), by removing the insignificant components.

$$Y_1 = 85.76 + 0.142A + 1.57B + 9.58C + 8.61D + 6.03AB + 0.87AC + 2.37AD + 2.99BC + 0.22BD + 2.38CD - 28.45C^2 + 1.83ABC + 0.33ABD - 0.51ACD - 1.31BCD$$

Table 4
Adequacy of the proposed models

Source	Sum of squares	df	Mean square	F value	p-Value	Remarks
Linear	6883.89	20	344.19	8668.43	< 0.001	
2FI	5964.68	14	426.05	10729.90	< 0.001	
Quadratic	135.66	10	13.57	341.66	< 0.001	Suggested
Cubic	49.48	2	24.74	623.12	< 0.001	Aliased
Pure error	0.1985	5	0.0397			

Table 5
ANOVA variance analysis for RB dye removal efficiency (R%)

Source	Sum of squares	df	Mean square	F value	p-Value	Remark
Model	9913.74	19	521.78	26179.74	<0.0001	Significant
A-A	0.3364	1	0.3364	18.38	0.0016	Significant
B-B	44.30	1	44.30	2222.68	<0.0001	Significant
C-C	1651.63	1	1651.63	82869.42	<0.0001	Significant
D-D	1333.55	1	1333.55	66910.03	<0.0001	Significant
AB	582.64	1	582.64	29233.72	<0.0001	Significant
AC	12.35	1	12.35	619.74	<0.0001	Significant
AD	89.72	1	89.72	4501.58	<0.0001	Significant
BC	143.21	1	143.21	7185.42	<0.0001	Significant
BD	0.7912	1	0.7912	39.70	<0.0001	Significant

CD	90.50	1	90.50	4540.63	<0.0001	Significant
A ²	0.0000	1	0.0000	0.0009	0.9771	Insignificant
B ²	0.0000	1	0.0000	0.0009	0.9771	Insignificant
C ²	2098.92	1	2098.92	1.053E+5	<0.0001	Significant
D ²	0.0001	1	0.0001	0.0075	0.9328	Insignificant
ABC	52.53	1	52.53	2635.83	<0.0001	Significant
ABD	1.76	1	1.76	88.15	<0.0001	Significant
ACD	4.32	1	4.32	216.66	<0.0001	Significant
BCD	27.57	1	27.57	1383.19	<0.0001	Significant
ABCD	49.48	1	49.48	2482.84	<0.0001	Significant
Residual	0.1993	10	0.0199			Insignificant
Lack of fit	0.0008	5	0.0002	0.0039	1.000	Insignificant
Pure error	0.1985	5	0.0397			
Cor. Total	9913.94	29				

After excluding the insignificant components, the reduced model was statistically tested using the analysis of variance, as shown in Table 5. The ANOVA results for RB dye removal showed a high model F_{value} of 40338.90 and a smaller P_{value} (<0.001). These values indicate that the reduced model was significant. On the other hand, the correlation coefficient determination ($R^2 = 0.99998$) and the adjusted determination coefficient ($R^2_{\text{Adj}} = 0.9999$) were very satisfactory, permitting the use of the reduced model for optimization of RB dye removal by EF process.

Effect of operating variables on RB removal

Figure 3 shows the individual effect of the variables. Linear constant and positive effects are observed for three variables: stirring speed (A) (Fig. 3a), oxygen flow (B) and supporting electrolyte (D) (Fig. 3b and 3d), respectively. The constant effect observed for stirring speed suggests that the RB dye removal is not affected by the mass transfer. However, the positive effect for both variables A and B resulted from the improved current intensity and, consequently, enhanced RB dye removal in accordance with Ohm's law. A significant amount of O_2 promotes the H_2O_2 production process, while a sufficient number of ions improve the solution conductivity.

A nonlinear relationship was observed between the current intensity (C) and the response. The efficiency of RB dye removal increased with the increase of current intensity from 0.2 to 0.356 A, attributed to the electro-regeneration of Fenton reagent's " Fe^{+2} and H_2O_2 ".¹⁰ However, any further increase in the current intensity could decrease the RB removal due to the generation of 'parasite' reactions of hydroxyl radicals, which is developed from fast electrode reactions, such as water electrolysis.¹⁴

Figure 4 illustrates the 3D surface plots derived from the quadratic polynomial model of the independent variable interactions. Figure 4 shows that the stirring speed variable, in association with the other variables, exhibits a nonlinear effect with the oxygen flow and current intensity. Furthermore, the intense agitation breaks up the oxygen bubbles, increasing the surface area of the bubbles and consequently enhancing the parasitic reactions, such as hydrogen peroxide oxidation at the anode (Eq. 14), and the reduction of hydrogen peroxide at the cathode (Eq. 16).¹⁵



However, the same behaviour of the current intensity effect was observed for the stirring speed and current intensity interaction, which reveals that the electrochemical reactions are not affected by the stirring speed. Moreover, the proportional relationship between the supporting electrolyte concentration and stirring speed is explained by the improvement in mass transfer. The 3D surface plots illustrating the interaction of current intensity with the other variables strongly depend on the evolution of the current intensity curve. According to Faraday's law, the current intensity is proportional to the accumulation of ferrous ions released from the sacrificial anode and the reduction of Fe^{3+} to Fe^{2+} (Eq. 4).⁹ Therefore, a higher current intensity up to 0.356 A provides more catalyst for the Fenton reaction. However, above this value, parasitic reactions may occur, affecting RB dye removal.^{15,42}



The linear effect of the simultaneous variation of oxygen flow and supporting electrolyte concentration was illustrated on the 3D surface plot interaction. In addition, this plot

demonstrates that the supporting electrolyte enhances the conductivity and accelerates the electron transfer in EF systems.

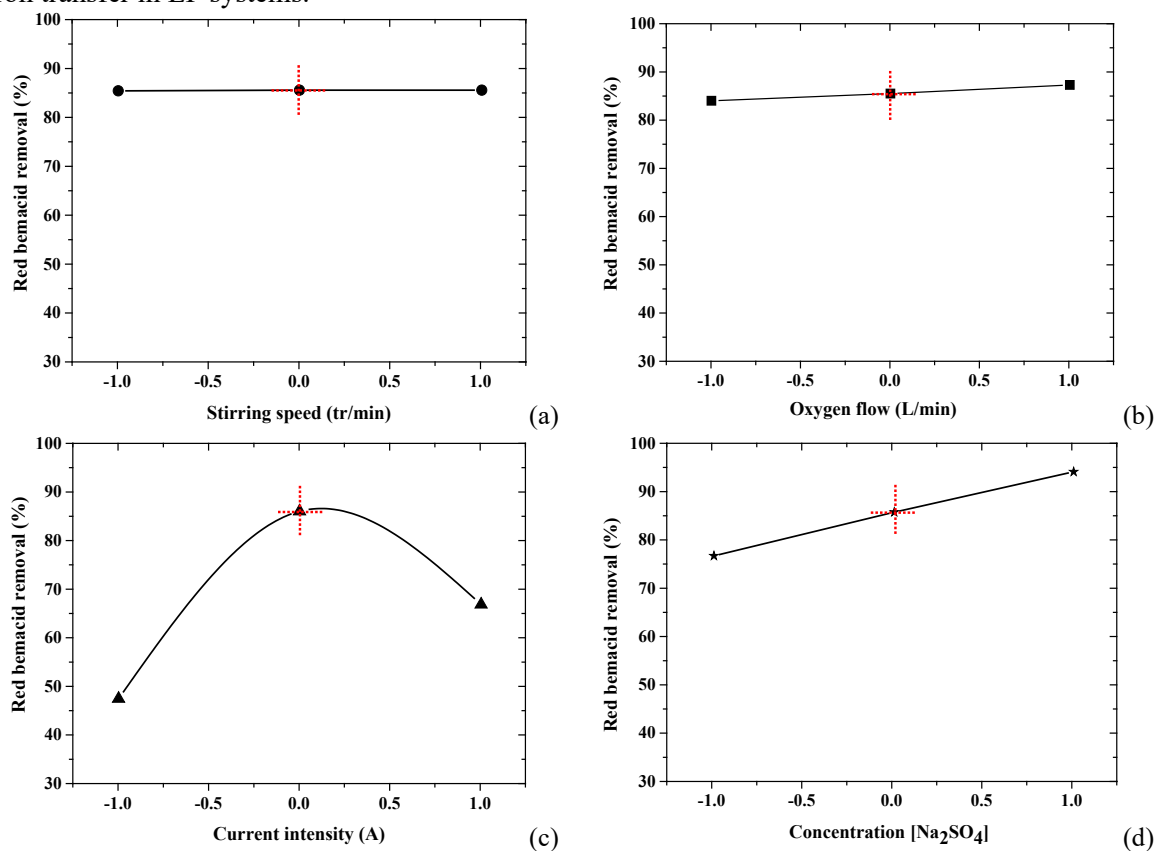


Figure 3: Individual effect of independent variables: (a) stirring speed, (b) oxygen flow, (c) current intensity, and (d) supporting electrolyte

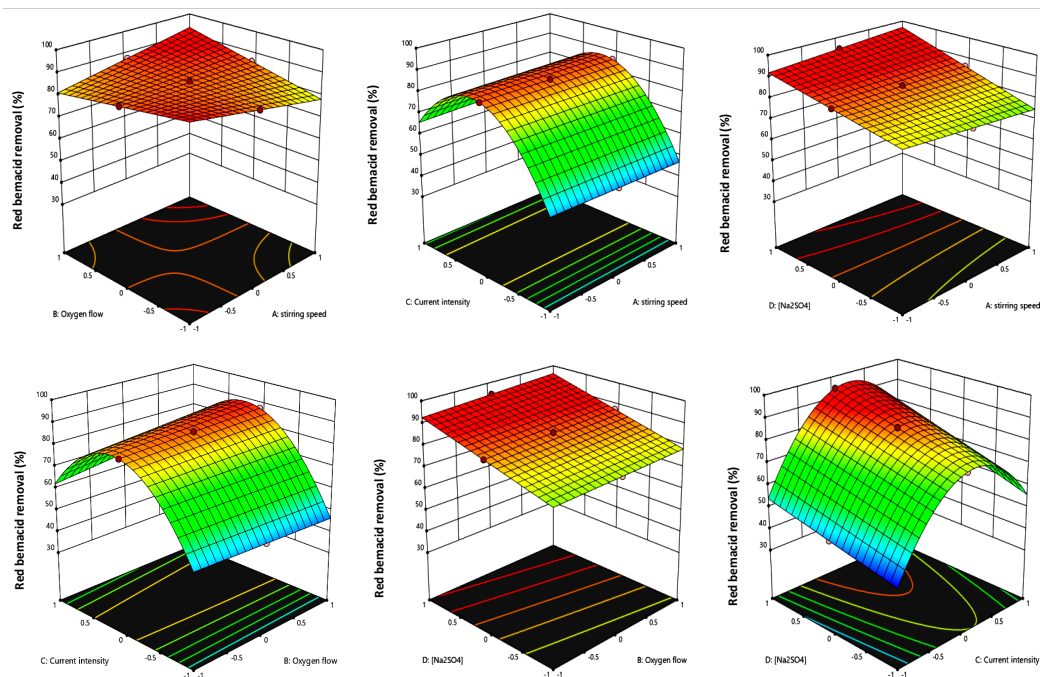


Figure 4: Response surfaces of RB dye removal for the most important pairs of variables

CONCLUSION

This study demonstrated the effectiveness of CCF in developing a suitable mathematical model for predicting the removal of RB dye by the EF process. The correlation coefficient determination ($R^2 = 0.99998$) and the adjusted determination coefficient ($R^2_{Adj} = 0.9999$), both close to 1, prove that the selected model is a promising tool for predicting the response accurately.

The CCF analysis not only provided insights into the individual effects of the variables, but also revealed the interactive effects through 3D surface plots for all pairs of variables. Among the variables, the current intensity factor was found to have a substantial effect on the production of Fenton reagents and, consequently, on RB dye removal.

Based on the analysis, the optimal conditions for achieving a satisfactory RB removal efficiency were determined. The analysis estimated an adequate RB removal efficiency of 94.51% under the following optimized parameters: a stirring speed of 205.09 rpm, oxygen flow rate of 0.20 L/min, current intensity of 0.306 A, and supporting electrolyte concentration of 0.09 M. Finally, the obtained results illustrate the successful optimization of EF process parameters for efficient RB dye removal and confirm the potential of CCD as a reliable tool for process modelling and optimization in wastewater treatment applications.

ACKNOWLEDGEMENTS: The authors would like to thank Pr. Umran Tezcan Un from Eskisehir Technical University for her helpful discussion and technical instruction.

REFERENCES

- 1 M. Teymori, H. Khorsandi, A. A. Aghapour, S. J. Jafari and R. Maleki, *Appl. Water Sci.*, **10**, 1 (2020), <https://doi.org/10.1007/s13201-019-1123-5>
- 2 T. M. Do, J. Y. Byun and S. H. Kim, *Catal. Today*, **295**, 48 (2017), <https://doi.org/10.1016/j.cattod.2017.05.016>
- 3 R. Rekik, M. Hamza, M. Jaziri and R. Abdelhedi, *Arab. J. Chem.*, **13**, 357 (2020), <https://doi.org/10.1016/j.arabjc.2017.05.001>
- 4 P. S. Vassileva, I. M. Uzunov and D. K. Voykova, *Cellulose Chem. Technol.*, **56**, 1117 (2022), <https://doi.org/10.35812/CelluloseChemTechnol.2022.56.100>
- 5 M. Visa, M. Cosnita, M. Moldovan, C. A. Marin and M. Mihaly, *Int. J. Environ. Res. Public Health*, **18**, 3887 (2021), <https://doi.org/10.3390/ijerph18083887>

- 6 N. Ouslimani and M. Maallem, *ISJAE*, **62**, 219 (2008)
- 7 K. Cruz-González, O. Torres-Lopez, A. M. García-León, E. Brillas, A. Hernández-Ramírez *et al.*, *Desalination*, **286**, 63 (2012), <https://doi.org/10.1016/j.desal.2011.11.005>
- 8 A. A. Alvarez-Gallegos and S. Silva-Martínez, in “Electro-Fenton Process. The Handbook of Environmental Chemistry”, edited by M. Zhou, M. Oturan and I. Sirés, Springer, Singapore, 2018, vol. 61, pp. 287-312, https://doi.org/10.1007/698_2017_73
- 9 M. Shoorangiz, M. R. Nikoo, M. Salari, G. R. Rakhshandehroo and M. Sadegh, *Process Saf. Environ. Prot.*, **132**, 340 (2019), <https://doi.org/10.1016/j.psep.2019.10.011>
- 10 P. H. Chang, Y. H. Huang, C. L. Hsueh, M. C. Lu and G. H. Huang, *Water Sci. Technol.*, **49**, 213 (2004), <https://doi.org/10.2166/wst.2004.0266>
- 11 M. Radwan, M. G. Alalm and H. Eletriby, *J. Water Process Eng.*, **22**, 155 (2018), <https://doi.org/10.1016/j.jwpe.2018.02.003>
- 12 H. Mohammadi, B. Bina and A. Ebrahimi, *Process Saf. Environ. Prot.*, **117**, 200 (2018), <https://doi.org/10.1016/j.psep.2018.05.001>
- 13 G. Divyapriya and P. V. Nidheesh, *ACS Omega*, **5**, 4725 (2020), <https://doi.org/10.1021/acsomega.9b04201>
- 14 R. Q. Al-Khafaji and A. H. A. Mohammed, *IOP Conf. Ser.: Mater. Sci. Eng.*, **518**, 062007 (2019), <https://doi.org/10.1088/1757-899X/518/6/062007>
- 15 N. Oturan and M. A. Oturan, in “Electrochemical Water and Wastewater Treatment”, edited by C. A. Martínez-Huitle, M. A. Rodrigo and O. Scialdone, Elsevier, Butterworth-Heinemann, 2018, pp. 193-221, <https://doi.org/10.1016/B978-0-12-813160-2.00008-0>
- 16 A. R. Khataee, M. Zarei and L. Moradkhannejhad, *Desalination*, **258**, 112 (2010), <https://doi.org/10.1016/j.desal.2010.03.028>
- 17 A. K. Abdessalem, N. Bellakhal, N. Oturan, M. Dachraoui and M. A. Oturan, *Desalination*, **250**, 450 (2010), <https://doi.org/10.1016/j.desal.2009.09.072>
- 18 V. V. Kuznetsov, *Russ. J. Gen. Chem.*, **84**, 525 (2014), <https://doi.org/10.1134/S1070363214030207>
- 19 M. Zhou, M. A. Oturan and I. Sires, in “Electro-Fenton Process. The Handbook of Environmental Chemistry”, edited by M. Zhou, M. Oturan and I. Sirés, Springer, Singapore, 2018, vol. 61, <https://doi.org/10.1007/978-981-10-6406-7>
- 20 A. Tabai, O. Bechiri, H. Ferdénache and M. Abbessi, *Synthèse: Revue des Sciences et de la Technologie*, **34**, 1 (2017), <https://www.ajol.info/index.php/srst/article/view/157233>
- 21 P. V. Nidheesh, H. Olvera-Vargas, N. Oturan and M. A. Oturan, in “Electro-Fenton Process. The Handbook of Environmental Chemistry”, edited by M. Zhou, M. Oturan and I. Sirés, Springer, Singapore, 2018, vol. 61, pp. 85-110, https://doi.org/10.1007/698_2017_72

- ²² E. Marlina, *E3S Web of Conferences*, **125**, 03003 (2019), <https://doi.org/10.1051/e3sconf/201912503003>
- ²³ P. V. Nidheesh and R. Gandhimathi, *Desalination*, **299**, 1 (2012), <https://doi.org/10.1016/j.desal.2012.05.011>
- ²⁴ W. Zhang, J. Chen, J. Wang, C. X. Cui, B. Wang *et al.*, *Water J.*, **13**, 128 (2021), <https://doi.org/10.3390/w13020128>
- ²⁵ C. T. Wang, W. L. Chou, M. H. Chung and Y. M. Kuo, *Desalination*, **253**, 129 (2010), <https://doi.org/10.1016/j.desal.2009.11.020>
- ²⁶ M. M. Ghoneim, H. S. El-Desoky and N. M. Zidan, *Desalination*, **274**, 22 (2011), <https://doi.org/10.1016/j.desal.2011.01.062>
- ²⁷ M. Panizza and G. Cerisola, *Water Res.*, **43**, 339 (2009), <https://doi.org/10.1016/j.watres.2008.10.028>
- ²⁸ K. M. Nair, V. Kumaravel and S. C. Pillai, *Chemosphere*, **269**, 129325 (2021), <https://doi.org/10.1016/j.chemosphere.2020.129325>
- ²⁹ A. R. Khataee, M. Safarpour, M. Zarei and S. Aber, *J. Mol. Catal. A. Chem.*, **363**, 58 (2012), <https://doi.org/10.1016/j.molcata.2012.05.016>
- ³⁰ M. Guo, M. Lu, H. Zhao, F. Lin, F. He *et al.*, *J. Hazard. Mater.*, **423**, 127033 (2022), <https://doi.org/10.1016/j.jhazmat.2021.127033>
- ³¹ H. He and Z. Zhou, *Crit. Rev. Environ. Sci. Technol.*, **47**, 2100 (2017), <https://doi.org/10.1080/10643389.2017.1405673>
- ³² M. A. Behnajady, N. Modirshahla and F. Ghanbary, *J. Hazard. Mater.*, **148**, 98 (2007), <https://doi.org/10.1016/j.jhazmat.2007.02.003>
- ³³ J. N. Hakizimana, B. Gourich, M. Chafi, Y. Stiriba, C. Vial *et al.*, *Desalination*, **404**, 1 (2017), <https://doi.org/10.1016/j.desal.2016.10.011>
- ³⁴ K. K. Salam, A. O. Arinkoola, E. O. Oke and J. O. Adeleye, *Petroleum Coal*, **56**, 19 (2014), https://www.vurup.sk/wp-content/uploads/dlm_uploads/2017/07/pc_1_2014_salam_245-3.pdf
- ³⁵ M. B. Kasiri and A. R. Khataee, *Desalination*, **270**, 151 (2011), <https://doi.org/10.1016/j.desal.2010.11.039>
- ³⁶ S. Choojit, T. Ruengpeerakul and C. Sangwichien, *Cellulose Chem. Technol.*, **52**, 247 (2018), [https://cellulosechemtechnol.ro/pdf/CCT3-4\(2018\)/p.247-257.pdf](https://cellulosechemtechnol.ro/pdf/CCT3-4(2018)/p.247-257.pdf)
- ³⁷ P. Kaur and R. Kaur, *Cellulose Chem. Technol.*, **55**, 1001 (2021), <https://doi.org/10.35812/CelluloseChemTechnol.2021.55.86>
- ³⁸ C. A. Floudas and V. Visweswaran, "Quadratic Optimization. Handbook of Global Optimization", 1995, pp. 217-269, https://doi.org/10.1007/978-1-4615-2025-2_5
- ³⁹ C. Sidney Santana, M. D. Nicodemos Ramos, C. C. Vieira Velloso and A. Aguiar, *Int. J. Environ. Res. Public Health*, **16**, 1602 (2019), <https://doi.org/10.3390/ijerph16091602>
- ⁴⁰ N. U. H. Khan, H. N. Bhatti, M. Iqbal and A. Nazir, *Zeitschrift für Physikalische Chemie*, **233**, 361 (2019), <https://doi.org/10.1515/zpch-2018-1194>
- ⁴¹ J. Fu, Y. Zhao and Q. Wu, *J. Hazard. Mater.*, **144**, 499 (2007), <https://doi.org/10.1016/j.jhazmat.2006.10.071>
- ⁴² S. Hammami, PhD Thesis, Environmental Sciences, Université de Marne la Vallée, France, 2008, <https://theses.hal.science/tel-00740155>